International Science and Technology Journal
المجلة الدولية للعلوم والتقنية

Volume 37 العدد
Part 1 المجلد

http://www.doi.org/10.62341/emaf0702

Received	2025/06/23	تم استلام الورقة العلمية في
Accepted	2025/07/19	تم قبول الورقة العلمية في
Published	2025/07/20	تم نشر الورقة العلمية في

Fuzzy Logic-Based Robust Control Design for PMSM Speed Regulation

Ezzaddine Ahmed[1], Mohammed Alrazqi[2], and Adel Ramadan[3]

[1]Department of Electrical and Electronic Engineering, Higher Institute of Science and Technology Awalad Ali –Tarhouna – Libya
ezzaddineahmed@gmail.com
[2]Department of Electrical and Electronic Engineering, Higher Institute of Engineering Technology – Zliten (HIETZ) – Libya
mohamedaalrazgi@gmail.com
[3]Department of Electrical and Electronic Engineering, Higher Institute of Science and Technology Tarhouna – Libya
Adel_rm81@yahoo.com

Abstract

This study proposes a robust speed control strategy for Permanent Magnet Synchronous Motor (PMSM) drives using a Fuzzy Logic Controller (FLC) integrated with field-oriented control (FOC). The conventional PI controller in the speed control loop is replaced with an FLC to enhance dynamic performance, while a hybrid Fuzzy Logic-PI Controller (FL-PIC) is employed in the current control loop to mitigate sensitivity to parameter variations. The proposed scheme ensures precise speed regulation through vector control representation, achieving accurate tracking of step and bidirectional speed changes with zero overshoot and negligible ripple. Simulation results demonstrate the system's rapid rejection of sudden load torque disturbances and robust performance under significant parameter mismatches. The controller maintains stable operation across low and high-speed ranges, with minimal steady-state distortion, confirming its resilience to parametric uncertainties, validating the reliability of the proposed FLC-based approach under non-ideal operational conditions.

Keywords; Fuzzy Logic Control (FLC), PMSM Drives, PI Controller, Field-Oriented Control.

http://www.doi.org/10.62341/emaf0702

تصميم تحكم قوي قائم على المنطق الضبابي لتنظيم سرعة المحركات التزامنية ذات المغناطيس الدائم

عزالدين احمد[1]، محمد الرازقي[2]، عادل رمضان[3]

[1]قسم الهندسة الكهربائية و الالكترونية، **المعهد** العالي للعلوم و لتقنية اولاد علي، ترهونة– ليبيا
ezzaddineahmed@gmail.com

[2]قسم الهندسة الكهربائية و الالكترونية، المعهد العالي للتقنيات الهندسية زليتن، زليتن– ليبيا
mohamedaalrazgi@gmail.com

[3]قسم الهندسة الكهربائية و الالكترونية، المعهد العالي للعلوم و التقنية ترهونة، ترهونة– ليبيا
Adel_rm81@yahoo.com

الملخص

تقترح هذه الدراسة استراتيجية فعّالة للتحكم في سرعة محركات المغناطيس الدائم المتزامنة (PMSM) باستخدام وحدة تحكم منطقية ضبابية (FLC) مدمجة مع نظام التحكم المجالي الموجه (FOC). استُبدلت وحدة التحكم التقليدية PI في حلقة التحكم بالسرعة بوحدة FLC لتحسين الأداء الديناميكي، بينما استُخدمت وحدة تحكم هجينة من نوع Fuzzy Logic-PI (FL-PIC) في حلقة التحكم بالتيار لتخفيف حساسية تغير البارامترات. يضمن النظام المقترح تنظيمًا دقيقًا للسرعة من خلال تمثيل التحكم المتجهي، مما يحقق تتبعًا دقيقًا لتغيرات السرعة التدريجية ولتغيرات السرعة ثنائية الاتجاه مع عدم تجاوز الحد الأقصى و بتموج ضئيل جداً يمكن إهماله. تُظهر نتائج المحاكاة قدرة النظام على الرفض السريع لاضطرابات عزم الحمل المفاجئة، وأداءً قويًا في ظل عدم تطابق كبير في البارامترات. تحافظ وحدة التحكم على تشغيل مستقر عبر نطاقات السرعات المنخفضة والعالية، مع أدنى حد من التشوه في الحالة المستقرة، مما يؤكد مرونتها و متانتها في مواجهة عدم اليقين البارامتري، ويثبت موثوقية النهج المقترح القائم على FLC في ظل ظروف تشغيل غير مثالية.

الكلمات المفتاحية: التحكم المنطقي الضبابي، المحركات التزامنية ذات المغناطيس الدائم، وحدة تحكم تناسبية تكاملية ، التحكم المجالي الموجه.

1. Introduction

Permanent Magnet Synchronous Motors (PMSMs) have gained prominence in the industrial sector due to their enhanced efficiency, elevated power density, low inertia, and high torque-to-inertia ratio.

http://www.doi.org/10.62341/emaf0702

Additionally, their significant air gap flux density, elimination of slip rings, and rapid dynamic response further contribute to their growing utilization in various applications. These properties make PMSMs very suitable for applications such as robotics and electric vehicles, where fast response is essential [1, 2].

In order to achieve accurate speed and/or torque control, Permanent Magnet Synchronous Motors (PMSMs) are typically powered by a voltage-fixed pulse-width modulation (PWM) inverter that is directly connected to the motor windings. The synchronization of the windings with the rotor position is essential and can be achieved through rotor position sensors or sensorless techniques. By selectively energizing specific stator windings in accordance with the rotor's position, a rotating magnetic field is generated, with only two of the three stator windings activated during each commutation cycle. This technique enables precise adjustments of the voltage and frequency supplied to the motor, allowing for rapid modifications to accommodate changes in speed and torque requirements [1, 3].

For speed and position regulation in Permanent Magnet Synchronous Motors (PMSMs), two predominant control methodologies are employed: Direct Torque Control (DTC) and Field Oriented Control (FOC). While DTC offers certain advantages, it is associated with drawbacks such as low speed stability, torque ripple, and sensitivity to parameter variations [4, 5]. Conversely, the Field Oriented Control (FOC) algorithm is commonly utilized in AC machines due to its effectiveness in managing Permanent Magnet Synchronous Motors (PMSMs) and associated drive systems [5]. However, the reliance on encoders, resolvers, Hall Effect sensors, or other mechanical position sensors can result in heightened maintenance expenses and diminished system robustness. Consequently, sensorless control methods have garnered significant attention in recent research [1, 4].

Field-Oriented Control (FOC) represents a fundamental methodology for regulating both synchronous and induction machines. It achieves decoupled control of torque and rotor speed, emulating the operational characteristics of a separately excited DC motor. In DC machines, independent control of the rotor's armature current and field excitation is facilitated by commutators and brushes. Conversely, AC machines—whether synchronous or asynchronous—exhibit a variable spatial relationship between the rotating stator magnetomotive force (MMF) and the rotor flux linkage under dynamic load conditions. This spatial variation

http://www.doi.org/10.62341/emaf0702

induces transient torque oscillations and suboptimal dynamic response. FOC circumvents this limitation by continuously estimating the instantaneous rotor flux angle. This estimation enables the precise alignment of the stator current vector within a rotor flux-oriented reference frame, maintaining the torque-producing current component (i_q) in quadrature (approximately 90 degrees) with the rotor flux linkage. This alignment ensures maximal torque production per ampere while permitting independent regulation of rotor speed. Effective FOC implementation necessitates accurate knowledge of the rotor flux position, typically obtained via a position sensor (e.g., encoder or resolver) or sensorless estimation techniques. This sensor data facilitates the transformation of three-phase stator currents into the rotor flux reference frame and the subsequent modulation of stator voltage phase and amplitude. This principle of controlling both the magnitude and spatial orientation of stator current vectors underpins the synonymous designation of FOC as "vector control" [6].

This study adopts a vector control algorithm to achieve high-performance control of Permanent Magnet Synchronous Motors (PMSMs). Conventionally, proportional-integral (PI) controllers are employed for both speed and current regulation. However, fixed-gain PI controllers exhibit significant sensitivity to parameter variations, load disturbances, and other dynamic uncertainties, necessitating continual adaptation of control parameters. This limitation may be addressed through adaptive control techniques such as Model Reference Adaptive Control (MRAC) for dynamic response [7], Sliding-Mode Control (SMC) for robustness against uncertainties [8], and self-tuning PI controllers that adjust their gains based on real-time performance, enhancing overall system stability and responsiveness [9]. Critically, the design of these controllers relies on an accurate mathematical model of the system. In practical applications, developing such a model is frequently challenging due to unquantifiable load variations, parameter uncertainties (e.g., from magnetic saturation or thermal drift), and external disturbances. To circumvent these inherent limitations of model-dependent approaches, fuzzy logic controllers have been increasingly utilized for motor control applications in recent research.

http://www.doi.org/10.62341/emaf0702

2. MATHEMATICAL MODEL OF PMSM

Within the rotor-aligned Park (d-q) reference frame, the fundamental electrical and mechanical equations governing a Permanent Magnet Synchronous Motor (PMSM) are expressed as follows[10]:

$$v_d = R_s i_d + \frac{d\lambda_d}{dt} - \omega_e \lambda_q \tag{1}$$

$$v_q = R_s i_q + \frac{d\lambda_q}{dt} + \omega_e \lambda_d \tag{2}$$

Here, v_d and $v_q$represent the stator voltage components along the direct (d) and quadrature (q) axes, respectively. Correspondingly, i_d and i_q are the stator current components aligned with these axes. R_s represents the stator winding resistance. The electrical angular speed ω_e, is defined as $\omega_e = d\theta_e/dt = P\omega_r$, where θ_e is the electrical rotor position, ω_r is the mechanical rotor angular speed, and P is the number of pole pairs.

The stator flux linkages in the d-q axes are defined as follows:

$$\lambda_d = L_d i_d + \lambda_f \tag{3}$$

$$\lambda_q = L_q i_q \tag{4}$$

In these expressions, L_d and L_q represent the synchronous inductances along the d-axis and q-axis, respectively, and λ_f signifies the permanent magnet flux linkage.

The mechanical dynamics of the rotor are governed by Newton's second law for rotation:

$$T_e = j\frac{d\omega_r}{dt} + B\omega_r + T_L \tag{5}$$

where T_e is the electromagnetic torque generated by the motor, J represents the rotor moment of inertia, B is the viscous friction coefficient, and T_L is the load torque applied to the rotor. The electromagnetic torque is produced through the interaction of stator currents and magnetic fluxes, defined by:

$$T_e = (3/2)P\left[\lambda_f i_q + \left(L_d - L_q\right) i_d i_q\right] \tag{6}$$

Equation (6) explicitly characterizes the electromagnetic torque production, comprising a component proportional to the permanent magnet flux λ_f and q-axis current i_q, and a reluctance torque component arising from magnetic saliency (L_d-L_q) and the product of d-axis and q-axis currents ($i_d i_q$). This torque relationship fundamentally determines the motor's dynamic electromechanical response under varying operational conditions.

http://www.doi.org/10.62341/emaf0702

3. SPEED CONTROL OF PMSM

Field-Oriented Control (FOC), synonymous with "vector control", is an advanced methodology for regulating AC machines by representing stator phase currents as space vectors within a rotating reference frame. This technique employs coordinate transformations, notably the Park transformation, to project the three-phase stator quantities – inherently sinusoidal and time-varying in the stationary (a-b-c) frame – onto a synchronously rotating (*d*-*q*) reference frame that aligns with the rotor flux vector. This transformation effectively creates a control structure similar to that of a separately excited DC machine. FOC operates by specifying two orthogonal current reference commands: the torque-producing component (i_q) aligned with the quadrature q axis and the flux-producing component (i_d) aligned with the direct d axis. By continuously regulating these transformed quantities, FOC achieves decoupled control of torque and flux, enabling precise management of instantaneous electrical dynamics during both steady-state and transient operation. This decoupling constitutes FOC's principal advantage: it effectively linearizes the motor's inherently coupled, nonlinear dynamics. Consequently, FOC transcends the bandwidth limitations inherent in conventional control approaches designed for time-varying AC quantities within the stationary frame, providing robust and accurate performance across the motor's entire operating envelope [6].

The control strategy implemented in this study employs Field-Oriented Control (FOC). Three-phase stator currents are measured and transformed into a two-axis stationary reference frame (α-β) using the Clarke transformation, yielding the orthogonal current components i_α and i_β. These stationary frame currents are then transformed into a rotor flux-aligned, synchronously rotating reference frame (*d*-*q*) via the Park transformation, producing the direct-axis current i_d and quadrature-axis current i_q. Dedicated current regulators (typically PI controllers) compare these transformed measured currents (i_d ,i_q) with their respective reference values (i_d*, i_q*), generating voltage command signals (v_d*, v_q*) in the rotating frame to minimize the tracking error. These *d*-*q* axis voltage commands are transformed back into the stationary (α-β) frame using the inverse Park transformation. The resulting (α-β) reference voltage vectors (v_α*, v_β*) are converted into three-phase voltages (v_a*, v_b*, v_c*). The resulting three-phase

http://www.doi.org/10.62341/emaf0702

voltages are subsequently fed into a pulse width modulation (PWM) block to generate the switching signals for the inverter power stages, as illustrated in Fig. 8. This FOC strategy achieves decoupled control of torque (i_q) and flux (i_d), ensuring precise, dynamic, and efficient operation of the Permanent Magnet (PM) motor across its entire operating range.

4. FUZZY LOGIC CONTROL OF PMSM

While conventional PI controllers remain prevalent for speed regulation tasks in PMSM drives, their performance can be significantly degraded by load disturbances, speed variations, and parameter uncertainties. To overcome these limitations and enhance dynamic performance, intelligent control strategies like Fuzzy Logic Control (FLC) have been effectively applied to Permanent Magnet (PM) drives. FLC is particularly advantageous due to its inherent simplicity, rapid response characteristics, and robustness against load variations and parameter changes. Motivated by the need for improved disturbance rejection and adaptability [2, 6]. This study employs a specifically designed Fuzzy Logic Controller both in the speed regulation loop and current controller loop of the PMSM drive. The proposed fuzzy logic-based vector control scheme of drive system has been comprehensively implemented within the MATLAB/Simulink environment. This platform allows for extensive simulation capabilities, enabling the study to validate the effectiveness of the proposed method under various speed and torque conditions.

A. STRUCTURE OF FLC

A fuzzy logic system operates through three sequential stages, as illustrated in Figure 1:

- **Fuzzification**: This initial step converts numerical (crisp) input values into membership grades representing their degree of belonging to the predefined linguistic fuzzy sets within the input variable's partition.
- **Inference Module:** This stage comprises two key components:

a) The Rule Base, containing a set of linguistic IF-THEN rules defining the system's behavior.

b) The Inference Engine, which evaluates the applicable rules based on the current fuzzified inputs and determines the resulting fuzzy output sets.

http://www.doi.org/10.62341/emaf0702

- **Defuzzification:** This final step converts the aggregated fuzzy output (the combined result of all fired rules) into a single, precise crisp numerical value suitable for control or decision-making [2, 3, 11].

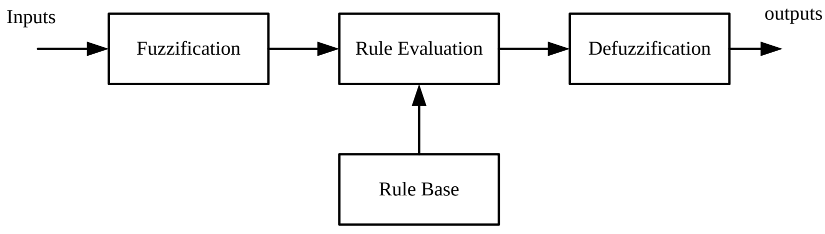

Figure 1. Structure of the Fuzzy Logic Control System.

B. FL-CONTROLLER FOR THE PM MOTOR

B-1. FLC FOR THE SPEED CONTROL LOOP

The speed control loop implements a fuzzy logic controller FLC with normalized speed error (***e***) and normalized speed error derivative (***ce***). The output is the change in the q-axis reference current **(Δi_q^*)** [3,10,11]. As illustrated in figure 2, membership functions define the linguistic variables for ***e, ce,*** and Δi_q^***.** To ensure effective operation, appropriate scaling factors (gains) are applied to both inputs and the output to normalize their ranges. The FLC core processes the fuzzified inputs ***e*** and ***ce*** through its rule base to determine the fuzzy output quantity $\Delta i_q{}^*$. This fuzzy output is then converted into a precise numerical value (Δi_q*) by the defuzzification process.

The input crisp variables are:

$$ce(n) = e(n) - e(n-1) \tag{7}$$

$$e(n) = \omega_r^*(n) - \omega_r(n) \tag{8}$$

The output of the FLC is the torque-producing reference current $i_q^*(n)$, which is obtained by integrating the change in the q-axis reference current $\Delta i_q^*(n)$ as follows:

$$i_q^*(n) = i_q^*(n-1) + G_3 . \Delta i_q^*(n) \tag{9}$$

http://www.doi.org/10.62341/emaf0702

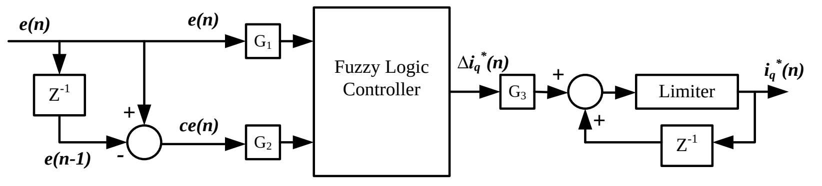

Figure 2. Diagram Components for a Fuzzy Logic Controller.

The design of membership functions (MFs) for speed error (***e***), change in speed error (***ce***), and output variable ($\boldsymbol{\Delta i_q}$*******) constitutes a core contribution of this work, as these MFs critically govern the fuzzy logic controller's (FLC) dynamic performance. Mamdani's inference method has been implemented for intuitive rule interpretation during fuzzification and employs the center of gravity method for precise output calculation during defuzzification as shown in Figure 3. Standard fuzzy rule base for FLC implementation is shown in Table 1. Linguistic variables follow the conventional 7-term set: Negative Big (NB), Negative Medium (NM), Negative Small (NS), Zero (ZE), Positive Small (PS), Positive Medium (PM), and Positive Big (PB). Critical parameters including scaling gains, MF boundary points, and fuzzy set granularity were refined through iterative simulation-based tuning, depending on fundamental knowledge and expert experience, where transient response metrics (overshoot, settling time) guided optimization toward robust performance across operating conditions. Figure 4. 3D control surface of the fuzzy speed controller, mapping normalized speed error (***e***) and change in error (***ce***) to the output current adjustment (***Δiq****).

Table 1. Rule-base matrix for Fuzzy Logic Speed Controller.

	Speed error (e)							
Error change rate (derivative)	$\boldsymbol{\Delta i_q}$*****	NB	NM	NS	ZE	PS	PM	PB
	NB	NB	NB	MB	NB	NM	NS	ZE
	NM	NB	NB	NB	NM	NS	ZE	PS
	NS	NB	NB	NM	NS	ZE	PS	PM
	ZE	NB	NM	NS	ZE	PS	PM	PB
	PS	NM	NS	ZE	PS	PM	PB	PB
	PM	NS	ZE	PS	PM	PB	PB	PB
	PB	ZE	PS	PM	PB	PB	PB	PB

http://www.doi.org/10.62341/emaf0702

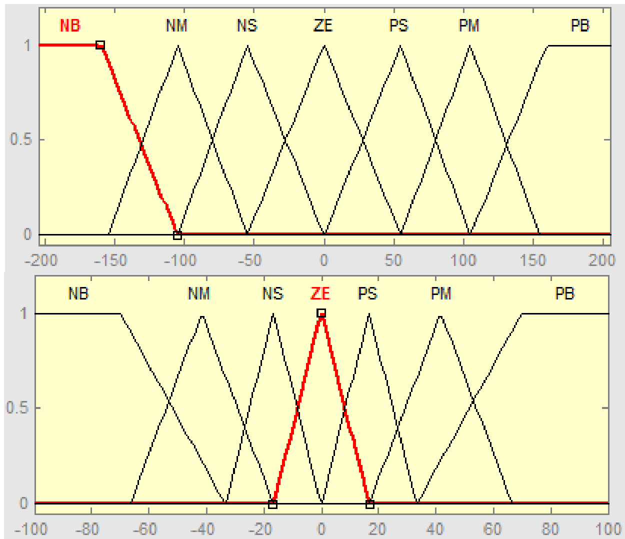

(a)

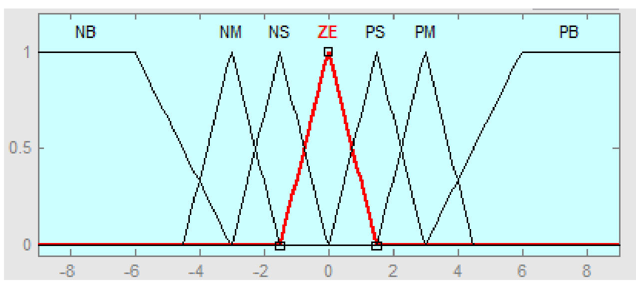

(b)

Figure 3. Membership functions (MFs) for:
(a) Normalized speed error (e) and its rate of change (ce).
(b) Command current adjustment (Δiq*) for speed-loop regulation.

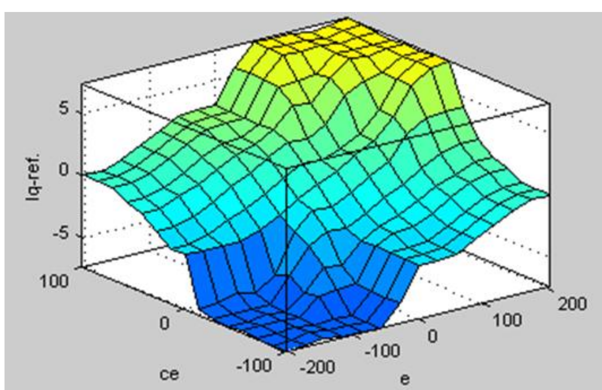

Figure 4. The output surface of speed controller.

http://www.doi.org/10.62341/emaf0702

B-2. FLC FOR THE CURRENT CONTROL LOOP

Conventional PI controller design for PMSMs relies on an accurate machine model, particularly the d-q axis reactance parameters. Obtaining precise values for these parameters is often challenging, complicating PI tuning. Furthermore, fixed-gain PI controllers exhibit sensitivity to parameter variations during operation. To address these limitations, a Fuzzy Logic-PI Controller (FL-PIC) replaces the standard PI controller within the inner current control loop (dual closed-loop control). The structure of this FL-PIC is illustrated in Figure 5. The inputs to the controller are [4, 12]:

- Stator Current Error (***e***): The difference between the reference stator current (**$i_{d/q}$***) and the measured stator current feedback (**$i_{d/q}$**).
- Change in Stator Current Error (***ce***): The derivative or discrete change of the error signal (***e***).

The FLC employs a standard two-input, two-output structure. Its outputs are:

a) Change in Proportional Gain (**Δk_p**)

b) Change in Integral Gain (**Δk_i**)

These output changes (**Δk_p, Δk_i**) dynamically adjust the parameters of a downstream PI controller block. The final output of the combined system is the reference stator voltage ($v_{d/q}$*) fed to the PWM modulation stage.

Scaling factors (gains) are applied to both inputs (***e, ce***) and outputs (**Δk_p, Δk_i**) to normalize their operating ranges prior to fuzzification and after defuzzification.

In the Mamdani-type fuzzy logic controller (FLC**)**, the input variables—**error (*e*)** and **change in error (*ce*)**—are first normalized via scaling factors to operate within the fuzzy inference system's predefined universe of discourse. The transformation is governed by:

$$\begin{aligned} E &= k_e e \\ CE &= k_c ce \end{aligned} \tag{10}$$

where:

E and *CE* are the **fuzzified inputs** (normalized error and change in error),

k_e and k_c are **scaling factors** that map physical signals to the normalized range.

e and ***ce*** are the raw input signals (typically $e = i_{d/q}^* - i_{d/q}$).

http://www.doi.org/10.62341/emaf0702

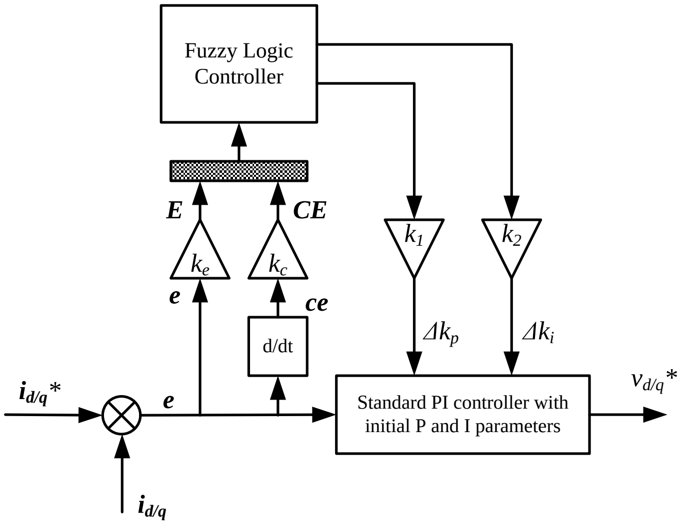

Figure 5. The block diagram of a FL-PIC for current loops.

The membership functions (MFs) typically triangular, trapezoidal, or Gaussian—assign membership degrees $\mu(E)$, $\mu(CE)\in[0,1]$ to quantify how much each crisp input belongs to linguistic terms.

To optimize computational efficiency in the current controller, both input domains (E, CE) intentionally constrained to five linguistic variables, because E and CE are smaller than that of speed controller. The linguistic variables span a normalized universe of discourse (-9,9), as shown in Figure 6 [4]. Membership functions (MFs) are structured to balance sensitivity and stability: Trapezoidal MFs bound both extremes of each input domain, ensuring robust handling of saturation conditions, and Triangular MFs characterize all intermediate sets, enabling precise resolution near the zero-error operating point. Controlled overlap between adjacent sets guarantees smooth output transitions.

This configuration intentionally reduces sensitivity to very small input values ($|E|$, $|CE| \approx 0$), minimizing unnecessary control adjustments during steady-state operation. Consequently, the initial proportional and integral gains ($\bar{k}_P$, $\bar{k}_i$) exhibit inherent stability—requiring minimal recalibration when errors remain within this near-zero regions.

The fuzzy rule base for PMSM current control as shown in table 2, implements a gain-scheduling strategy to balance dynamic response and steady-state performance, guided by three core principles [4, 12]:

http://www.doi.org/10.62341/emaf0702

- **Large errors** (|*E*| large): Prioritize rapid response by selecting larger Δk_p while suppressing Δk_i to limit integral windup and reduce overshoot.
- **Medium errors** (|*E*| or |*CE*| medium): Optimize transient behavior with moderate Δk_p while increasing Δk_i to enhance steady-state tracking and disturbance rejection.
- **Small errors** (|*E*| and |*CE*| small): Maximize precision with aggressive Δk_p and Δk_i to minimize steady-state error and accelerate convergence.

Table 2. Rule-base matrix for the Fuzzy Logic-PI Controller.

		Current error (e)				
Error change rate (derivative)	**Δkp/Δki**	NM	NS	ZE	PS	PM
	NM	PM/NM	PM/NM	PS/NS	ZE/ZE	ZE/ZE
	NS	PM/NS	PM/NS	ZE/ZE	ZE/ZE	NS/PS
	ZE	PS/NS	PS/NS	ZE/ZE	NS/PS	NS/PS
	PS	PS/ZE	ZE/ZE	NS/PS	NS/PS	NS/PM
	PM	ZE/ZE	ZE/ZE	NM/PS	NM/PM	NM/PM

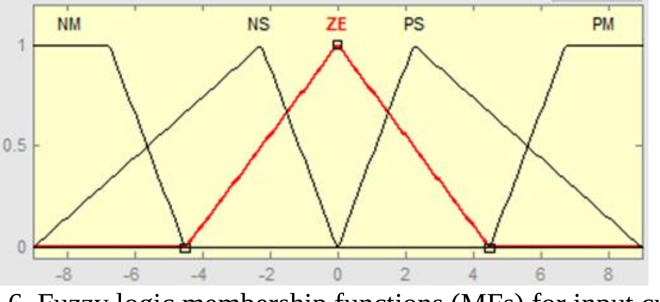

Figure 6. Fuzzy logic membership functions (MFs) for input current tracking error (e), error derivative (ce), and Output control variables (*Δkp, Δki*).

The current controller employs a non-uniform membership function (MF) distribution, with increased density near the origin, to enhance steady-state tracking precision. This design choice improves fine-grained error correction when operating near the reference set point. Fig. 7 illustrates the resulting output surface of the fuzzy inference system, demonstrating the nonlinear control action generated by the rule base.
The scaling factors *ke* and *kc* normalize the physical inputs ***e*** (error) and ***ce*** (error change rate) into the fuzzy variables *E* and *CE*, respectively, mapping them to the normalized domain. These factors function analogously to proportional and integral gains in conventional PI control, critically influencing closed-loop stability, damping characteristics, and oscillation suppression.

http://www.doi.org/10.62341/emaf0702

Consequently, their selection requires careful consideration. Given the absence of flux-weakening requirements in this application, ke and k_c are defined as [4]:

$$k_e = \frac{1}{e_{max}} \tag{11}$$

$$k_c = \frac{1}{ce_{max}} \tag{12}$$

where e_{max} and ce_{max} represent the maximum anticipated absolute values of ***e*** and ***ce*** respectively, determined empirically through dynamic simulation studies under worst-case operating conditions. Subsequent output scaling factors k_1 and k_2 convert the initial gain adjustments into the final incremental values ***Δkp*** and ***Δki.***

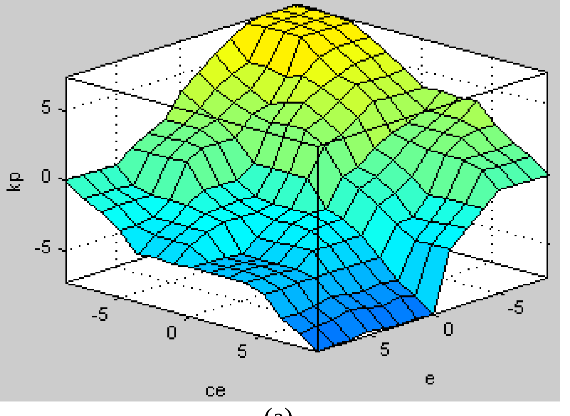

(a)

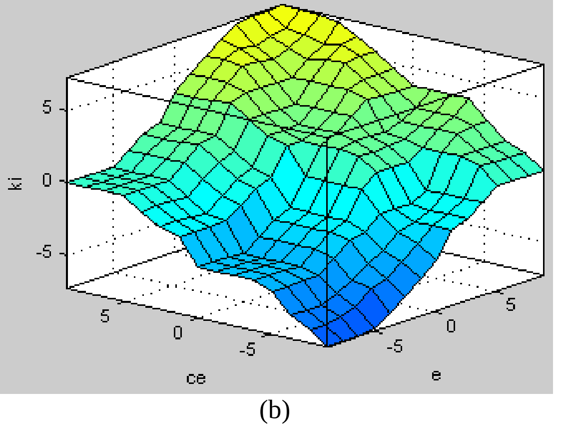

(b)

Fig. 7. The output surface of current controller, (a) *Δkp*, (b) *Δki*.

5. SIMULATION RESULTS

Figure 8 depicts the architecture of the control system, structured into two primary feedback loops: an outer loop responsible for speed regulation and an inner loop focused on regulating the d- and q-axis

http://www.doi.org/10.62341/emaf0702

stator currents. The outer speed controller utilizes a Fuzzy Logic Controller (FLC) to process the speed error signal and produce the torque-generating current command i_q*. To ensure appropriate field orientation, the flux- generating current command, i_d* is maintained at zero. The inner current control loop utilizes a Fuzzy Logic-PI Controller (FL-PIC) operating within the estimated rotor reference frame. This configuration effectively decouples cross-coupling dynamics and compensates for back-electromotive force (back-EMF) disturbances [13].
The Fuzzy Logic Controller discussed in this paper was analyzed within the MATLAB/Simulink environment. The motor model employed the parameters specified in Table 3.

TABLE-3. Overview of Motor Performance Parameters

Rated power	2.2 kw
Rated voltage V_N	380V
Rated current I_N	4.1A
Rated speed	1500 r/min
Rated torque T_N	15.0 Nm
Number of pole pairs P	3
Stator resistance R_s	3.61Ω
Direct axis inductance L_d	0.037H
Quadrature inductance L_q	0.052H
Flux of permanent magnet λ_f	0.555 Vs
Total moment of inertia	0.015kgm^2

Figure 9 presents simulation results obtained under no-load conditions, demonstrating the system's response to a step change in reference speed from zero to the rated value of 1500 rpm at t = 0 sec. The rotor speed exhibits smooth and accurate tracking of the reference profile during the acceleration phase, with no overshoot, and negligible speed ripple observed throughout steady-state operation.

Figure 10 presents simulation results under loaded conditions, demonstrating the system response to a step change in reference speed from zero to 1000 rpm at t = 0 sec.

http://www.doi.org/10.62341/emaf0702

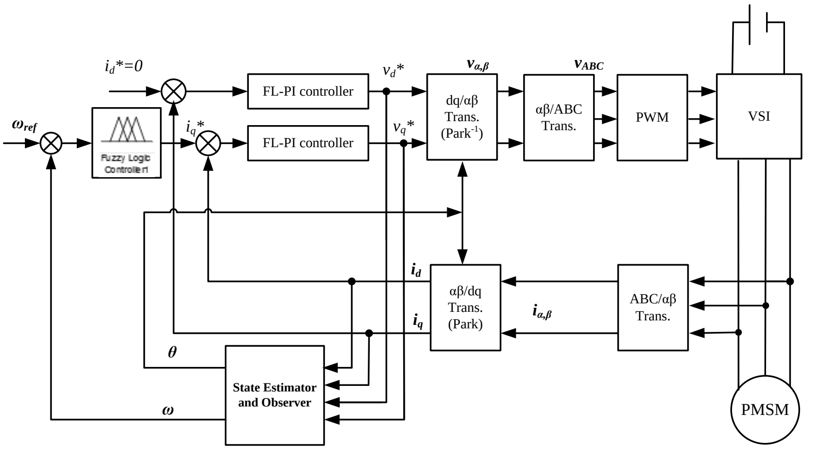

Figure 8. Schematic Representation of the Proposed Fuzzy-logic Control Scheme.

A sudden load torque step from 0 Nm to the rated torque of 15 Nm is applied at t = 0.6 sec. The load disturbance causes a minimal transient deviation in rotor speed. The controller rapidly rejects this disturbance, restoring the speed to its reference value with small steady-state error, while Fig. 11 displays the electromagnetic torque response to a sudden step change in load torque.

Figure 12 illustrates the speed response under nominal load torque during stepwise reference speed variations. Initially, the reference speed increased from zero to 1300 rpm at t = 0 sec, followed by a drop to 650 rpm at t = 0.2 sec, a rise to 1300 rpm at t = 0.5 sec, and finally returning to 650 rpm at t = 0.8 sec. The system response demonstrates precise tracking of these aggressive bidirectional step changes with minimal transient deviation and zero steady-state error. This performance highlights the control algorithm's robustness and responsiveness to rapid reference variations under load, confirming its effectiveness in dynamic speed regulation.

Figure 13 assesses the reliability of the proposed control scheme under significant motor parameter mismatches: winding resistance was increased by 20% ($R_s \rightarrow 1.2R_s$), flux linkage was reduced by 10% ($\lambda_f \rightarrow 0.9\lambda_f$), and the moment of inertia was doubled ($j \rightarrow 2j$). Despite these intentional modeling errors, the system effectively tracks a step reference speed change from zero to 1000 rpm at t = 0 sec. The rotor speed response exhibits negligible steady state deviation and maintains accurate regulation across both low and

http://www.doi.org/10.62341/emaf0702

high-speed operation. Minimal steady-state distortion confirms the controller's robustness to parametric uncertainties, validating its resilience under non-ideal operational conditions.

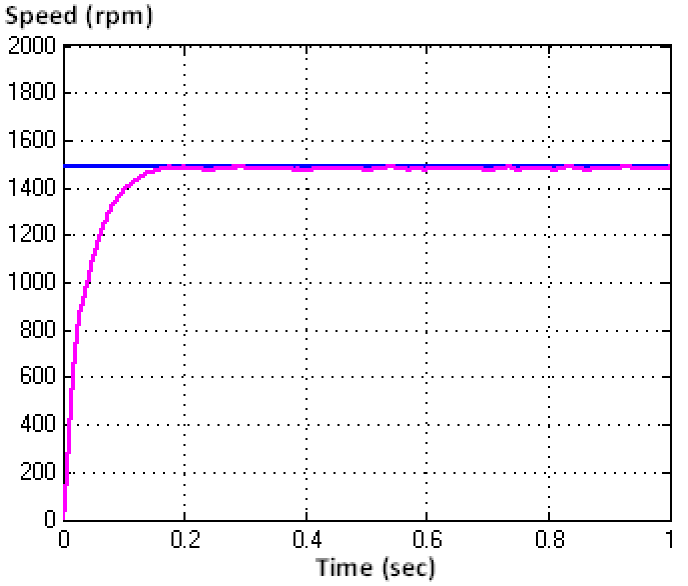

Figure 9. Rated rotor speed with no load.

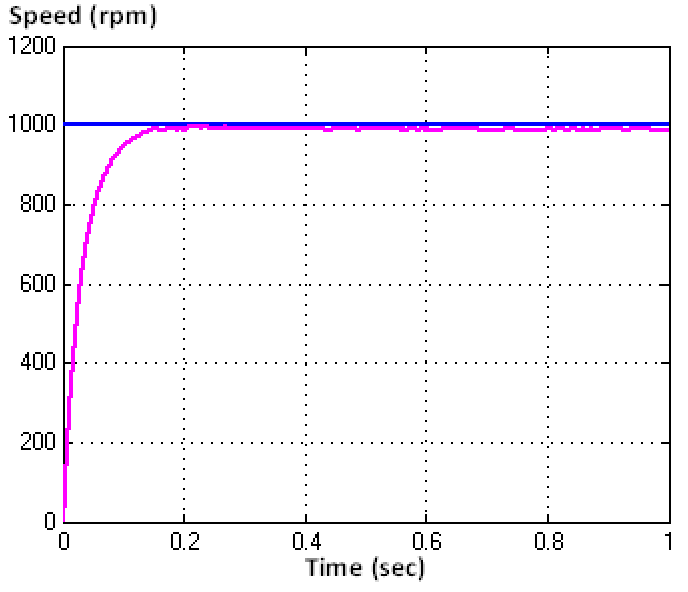

Figure 10. Speed response with a step change in load torque at 0.6 sec.

http://www.doi.org/10.62341/emaf0702

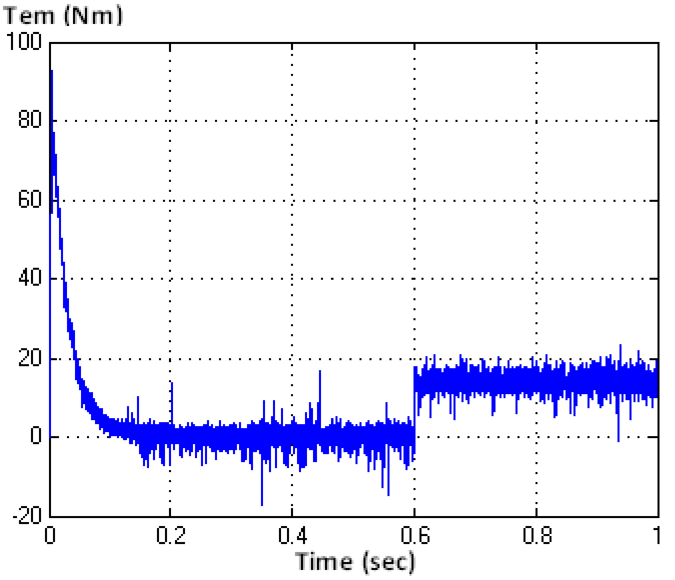

Figure 11. Electromagnetic torque response to a step change in load torque at 0.6 sec.

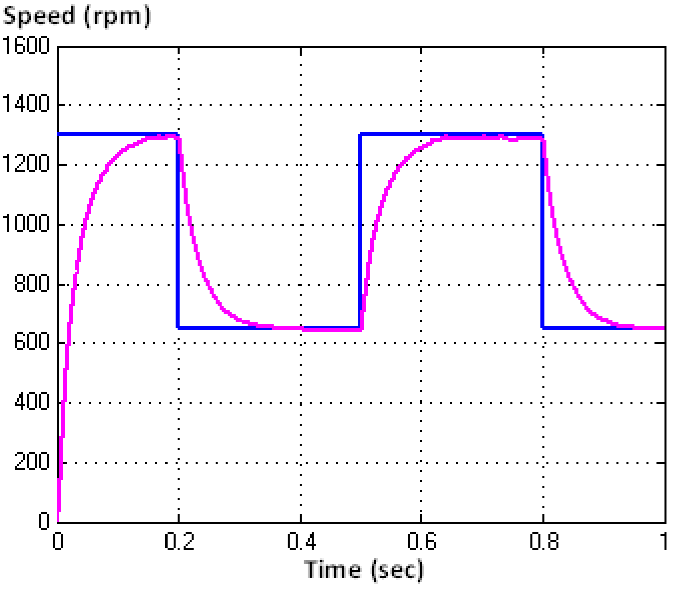

Figure 12. Speed response under nominal load torque during bidirectional reference speed variations.

http://www.doi.org/10.62341/emaf0702

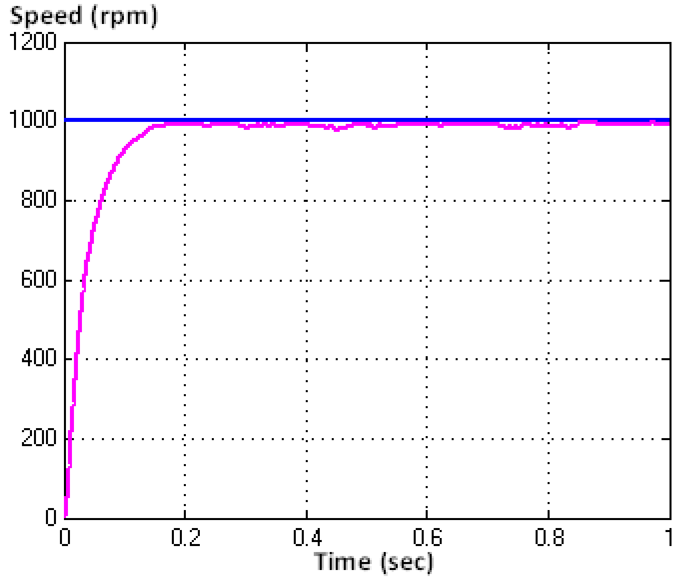

Figure 13. Speed response with mismatched Parameters.

6. CONCLUSION

The proposed Fuzzy Logic-based vector control scheme achieves precise speed regulation in a permanent magnet synchronous motor (PMSM) drive across a wide operating range. Simulation results demonstrate exact tracking of step and bidirectional speed changes with zero overshoot and negligible ripple. Additionally, the system exhibits rapid rejection of sudden load torque disturbances and maintains robust performance under significant parameter mismatches. The rotor speed remains accurately regulated at both low and high speeds, confirming the controller's effectiveness under varying conditions. Furthermore, minimal steady-state distortion underscores the scheme's robustness against parametric uncertainties, validating its reliability in non-ideal operational environments.

REFERENCES

[1] E. Ahmed, O. Montsr, and M. Alrazqi, "Model Reference Adaptive System for Speed Estimation of Permanent Magnet Synchronous Motors," *The second scientific conference for science and technology*. vol. 33, No. 9, pp. 09–25, Zliten-Libya 27-28 Nov 2024.

[2] I. Bouguenna, A. Tahour, R. Kennel, and M. Abdelrahem, "Multiple-Vector Model Predicative Control with Fuzzy logic for PMSM," *IEEE. Trans. Power Electron Electric Drive*

http://www.doi.org/10.62341/emaf0702

System. Energies 2021, 14, 1727. https://doi.org/10.3390/en14061727, 20 March 2021.

[3] P. T. M. Sahridayan, and R. Gopal, “Modeling and analysis of field-oriented control based permanent magnet synchronous motor drive system using fuzzy logic controller with speed response improvement,” *International Journal of Electrical and computer Engineering* . vol. 12, No. 6, pp. 1065–1073, Dec. 2022.

[4] Z. Liu, J. Nie, H. Wei, L. Chen, X. Li, and M. Lv, “Switched PI Control Based MRAS for Sensorless Control of PMSM Drive Using Fuzzy-Logic-Controller,”. *IEEE open journal of Power Electronics.* vol. 3. pp. 368-381, 13 June 2022.

[5] S. Murshid, and B. Singh, “Implementation of PMSM drive for a solar water pumping system*,” IEEE. Trans. Ind. App*l., vol. 55, No. 5, pp. 4956-4964, Sep./Oct.2019.

[6] A. Kushwaha, and V. Pathak, “Fuzzy Logic Based Speed Control of Electric Vehicle Driven by PMSM,” *International Journal of Creative Research Thoughhts (IJCRT)*. vol. 12, Issue 12, Dec. 2024. pp. 711–723, 2024.

[7] H. Sugimoto, S. Tamai, “Secondary resistance identification of an induction motor applied model reference adaptive system and its characteristics,” *IEEE Trans. Industry Applications IA-23*, pp. 296–303, 1987.

[8] C.-Y. Won, D. H. Kim, B. K. Bose “An induction motor servo system with improved sliding mode control,” *In: Proc. IEEE IECON 1992,* pp. 60–66, 1992.

[9] J. C. Hung, “Practical industrial control techniques,” *In: Proc. IEEE IECON 1994*, pp. 7–14, 1994.

[10] P. Kumar, and A. Tomer, “Modelling & Simulation of PMSM Drive with Fuzzy Logic Controller,” International Journal of Modern Engineering Research (IJMER). vol. 3, Issue 4, Aug. 2013. pp. 2492–2497, 2013.

[11] B. Shikkewal, and V. Nandanwar, “Fuzzy Logic Controller for PMSM,” *International Journal of Electrical and Electronic Engineering (IJEEE)*. vol. 1, Issue 3, pp. 73–78, 2012.

[12] A. M. Kassem, and A. M. Yousef, “Fuzzy-Logic Based Self-Tuning PI Controller for High–Performance Vector Controlled Induction Motor Fed By PV-Generator,” *Journal of Engineering Sciences*, Assiut University, vol. 40, No. 4, pp.1179-1193, July 2012.

http://www.doi.org/10.62341/emaf0702

[13] F. B. Blanco, M. W. Degner, and R. D. Lorenz, "Dynamic Analysis of Current Regulators for AC Motors using Complex Vectors," *IEEE Trans. On Indust. Appli*. vol. 35, No. 6, pp. 1424–1432, Nov/Dec. 1999.